

Chemometrics—Assisted Fluorimetry for the Rapid and Selective Determination of Heavy Polycyclic Aromatic Hydrocarbons in Contaminated River Waters and Activated Sludges

Santiago A. Bortolato, Juan A. Arancibia, and Graciela M. Escandar*

Instituto de Química Rosario (CONICET-UNR), Facultad de Ciencias Bioquímicas y Farmacéuticas, Universidad Nacional de Rosario, Suipacha 531 (2000) Rosario, Argentina.

S Supporting Information

ABSTRACT: The most concerned polycyclic aromatic hydrocarbons (PAHs) benzo[*a*]pyrene, dibenz[*a,h*]anthracene, chrysene, benzo[*b*]fluoranthene, benzo[*k*]fluoranthene and benz[*a*]anthracene were simultaneously determined in the presence of other 10 interfering PAHs, applying second-order multivariate calibration to the data obtained with a flow-through optosensor interfaced to a fast-scanning spectrofluorimeter. Using a sample volume of 2.5 mL, detection limits in the range 5–115 ng L⁻¹ were obtained in interfering samples, with a sample frequency of ca. 15 samples per hour, and with a minimum use of organic solvents, competing very favorably with chromatographic methods. The significance of this study lies in the solution of the quantitative analysis problem of six PAHs in real matrices of unknown composition. The unfolded partial least-squares/residual bilinearization (U-PLS/RBL) algorithm showed the best performance in resolving the complex studied system.

INTRODUCTION

Polycyclic aromatic hydrocarbons (PAHs) are ubiquitous environmental pollutants of both natural and anthropogenic origin, having to measurable background exposure levels in the general population. PAHs exposure in humans is associated with serious diseases, among which the most concerning one is cancer. The toxicity of PAHs depends on their molecular structure, with cancer associated to the so-called heavy PAHs (those bearing more than four benzene rings).¹ The United States Environmental Protection Agency (USEPA) considers benzo[*a*]pyrene (BaP), dibenz[*a,h*]anthracene (DBA), chrysene (CHR), benzo[*b*]fluoranthene (BbF), benzo[*k*]fluoranthene (BkF), and benz[*a*]anthracene (BaA) as probable human carcinogens based on evidence in animals.² On the other hand, according to the International Agency for Research on Cancer (IARC), BaP belongs to group 1 (carcinogenic to humans), DBA belongs to group 2A (probably carcinogenic to humans), and CHR, BbF, BkF, and BaA are included in the 2B group (possibly carcinogenic to humans).³ It is important to remark that BaP (group 1) is highly toxic even at very low concentrations, and thus maximum admitted level in environmental and food samples has been regulated in different countries.¹ In any case, the adverse effects of heavy PAHs on wildlife and humans are evident, justifying the efforts of regulatory agencies to monitor and control their presence in the environment.

In a previous work, we developed a nylon-phase extraction method coupled to excitation–emission fluorescence matrices (EEFMs) to simultaneously quantify BaP and DBA, the most harmful PAHs, at ng L⁻¹ levels.⁴ The latter work demonstrated the ability of unfolded partial least-squares coupled to residual bilinearization (U-PLS/RBL) to resolve the system even in the presence of other PAHs which produced a significant interference

in the analysis. As is well-known, some second-order algorithms allow the determination of target analytes in the presence of other unexpected components which can be present in complex real samples, but not in the calibration set. This property, known as the “second-order advantage”, allows working without the necessity of removing interferences before the analysis.⁵

Because of the growing interest on the application of chemometric methods to environmental analysis,⁶ and pursuing a more ambitious objective, the potentiality of second-order chemometric analysis was evaluated in the present work for a system containing more analytes and spectral interferences than in previous works. Specifically, the simultaneous determination of the six heavy-PAHs mentioned above, presenting significantly overlapped fluorescence spectra, was performed in the presence of 10 additional PAHs which strongly interfere with the analytes, namely benzo[*g,h,i*]perylene (BghiP), indeno[1,2,3-*cd*]pyrene (IcdP), acenaphthylene (ACEN), anthracene (ANT), fluoranthene (FLT), phenanthrene (PHEN), pyrene (PYR), benzo[*e*]pyrene (BeP), coronene (COR), and azulene (AZU). The tested algorithms were U-PLS/RBL,^{7,8} multidimensional partial least-squares⁹ coupled to RBL (N-PLS/RBL) and parallel factor analysis (PARAFAC).¹⁰ Both the sampling rate and sensitivity were improved by using a flow-through optosensing system.¹¹ Optosensors based on flow injection solid-matrix luminescence (FI-SML) using commercial supports for the retention of several PAHs have already been proposed.^{12–14} Since PAHs show similar spectral properties, a relevant problem to this methodology

Received: August 16, 2010

Accepted: December 12, 2010

Revised: December 10, 2010

Published: December 31, 2010

is the lack of selectivity when multicomponent samples are investigated. Although the use of molecularly imprinted polymers as solid-supports has been recently recommended for improving the selectivity of PAH analysis, this latter approach is only suitable for the determination of a single component in a mixture.¹⁵

Different commercial solids were probed for PAH retention, and the experimental parameters affecting the method sensitivity were optimized. The prediction capability of each employed algorithm was analyzed and discussed. The method was successfully applied to the determination of the evaluated PAHs in river waters sampled at places close to local industries, and also in activated sludges used in the treatment of industrial wastes from a petrochemical plant.

MATERIALS AND METHODS

Reagents and Solutions. Analytical reagent grade chemicals were used for the preparation of all solutions. All PAHs and Amberlite XAD-7 HP (20–60 mesh) were purchased from Aldrich (Milwaukee, WI). Methanol and acetonitrile were obtained from Merck (Darmstadt, Germany). Silica gel 100 C18-bonded phase (0.040–0.063 mm particle size) was purchased from Fluka (Buchs, Switzerland). Amberlite XAD-4 was obtained from SUPELCO (Bellefonte, PA). Stock solutions of all PAHs of about 1000 $\mu\text{g mL}^{-1}$ were prepared in acetonitrile. From these solutions, more diluted acetonitrile solutions were obtained. Working water-acetonitrile (50% v/v) solutions were prepared immediately before their use.

Apparatus. A Varian Cary-Eclipse luminescence spectrometer (Varian, Mulgrave, Australia) equipped with a xenon flash lamp was used to measure the optosensor response and to obtain the EEFMs. A Gilson Minipuls-3 peristaltic pump (Villiers-Le-Ber, France), two six-port injection valves, and a 25 μL inner volume quartz flow-through cell (Hellma 176.052-QS, Müllheim, Germany) packed with 25 mg of silica gel C18-bonded phase were employed to setup the FIA manifold. PVC tubing of 0.76 mm i.d. was used for all connections. Gas chromatography–mass spectrometry (GC–MS) analysis was carried out on a Perkin-Elmer (Norwalk, CT) AutoSystem XL gas chromatograph coupled to a Perkin-Elmer Turbomass mass spectrometer, equipped with vacuum Edwards RV3 and turbomolecular Edwards EXT 250 pumps. Chromatographic separation was performed by using a VF-1 ms (100% polydimethylsiloxane) column (30 m \times 0.25 mm i.d.) from Varian (Middelburg, Nederland). The samples were analyzed in selected-ion mode, run with an electron impact source. Upon positive identification of each specific compound, final quantification was performed using external calibration.

Synthetic samples. A calibration set of 14 samples containing the six studied PAHs in water-acetonitrile 50% v/v solutions was prepared from the diluted acetonitrile solutions. Twelve samples of the set corresponded to the concentrations provided by a Plackett-Burman design, and the remaining two samples corresponded to a blank solution and to a solution containing all the studied PAHs at an average concentration. The tested concentrations were in the ranges 0–300 ng L^{-1} for BaP and BkF, 0–1600 ng L^{-1} for DBA, 0–1000 ng L^{-1} for BaA, and 0–500 ng L^{-1} for BbF and CHR. Fluorescence–concentration linearity was confirmed for each analyte up to the maximum concentrations assayed and under the established working conditions.

A validation test set of 25 samples was prepared employing concentrations different from those used for calibration and

following a random design. Thirty six additional test samples containing random concentrations of both analytes and 10 interferences were prepared. The maximum concentrations of the interferences in these latter samples were 1×10^4 , 2.5×10^4 , 1×10^6 , 6×10^5 , 4×10^4 , 6×10^5 , 4×10^4 , 3×10^5 , 1×10^3 , and $6.25 \times 10^5 \text{ ng L}^{-1}$ for BghiP, IcdP, ANT, ACEN, FLT, PHE, PYR, BeP, COR, and AZU, respectively.

All samples were subjected to the flow–injection procedure and the obtained EEFMs were then analyzed with second-order multivariate calibration.

Real Samples. Paraná River water samples were collected near zones with profuse industrial activity. These river samples were filtered through filter paper to remove suspended sediments and solid materials. Solid-phase extraction (SPE) using SPE C18 cartridges from Supelco (Sigma-Aldrich, St. Louis, MO) was applied before the water analysis, following the method suggested in the literature.¹⁶ For the chromatographic measurement, 1000 mL of water were percolated to the conditioned cartridge under vacuum pump. After the elution of the retained organic compounds with 10 mL of acetonitrile, the solvent was evaporated, the solutions were reconstituted with 100 μL of dichloromethane, filtered through a 0.45 μm regenerated cellulose filter and injected in the GC–MS apparatus. The preconcentration factor for the chromatographic analysis was 10 000.

For the optosensor procedure, 20.0 mL of filtered river water were percolated through the cartridge and the elution was performed with 5.00 mL of acetonitrile. This solution was treated with an equal volume of water in order to obtain a 50% v/v acetonitrile:water solution, and subjected to the corresponding flow–injection analysis. In this way, the preconcentration factor was 2, highlighting the significant sensitivity of the applied method.

Activated sludge samples were obtained from a local petroleum refinery. Each sample was centrifuged at 7000 rpm during 10 min. The aqueous phase was separated and the residue was filtered in vacuum. The dry material (5.00 g) was then extracted with 5.00 mL of dichloromethane. This organic phase was filtered through regenerated cellulose and injected in the GC–MS. On the other hand, due to the high PAH content in this type of samples, dilutions steps were required to apply the presently proposed method. The dichloromethane solution was evaporated and reconstituted with 5.00 mL of acetonitrile. From this solution, more diluted acetonitrile solutions were prepared and, finally, a 50% v/v acetonitrile:water solution was obtained and subjected to the flow-injection system. All procedures were performed in duplicate.

Procedure. Two milliliters and a half of sample solution were inserted into the carrier stream (water) and pumped through the flow system at a flow rate of 2.0 mL min^{-1} . The luminescence spectrometer was first setup in its kinetic mode, using excitation and emission wavelengths of 300 and 408 nm, respectively, excitation and emission slit widths of 5 nm and photomultiplier sensitivity of 600 V. The PAHs arrive to the cell filled with the C18 solid support, where they are retained and the fluorescence signal is read. When the maximum fluorescence signal is reached, the flow is stopped, the fast-scanning spectrofluorimeter is setup in its scan 3D mode, and the corresponding EEFM is recorded using excitation and emission ranges of 250–346 nm (each 2 nm) and 350–490 nm (each 2 nm), respectively, at a scanning rate of 9600 nm min^{-1} . After these measurements, the kinetic mode is selected again, the flow is restored, and the analytes are desorbed with 500 μL of methanol, which are injected by means

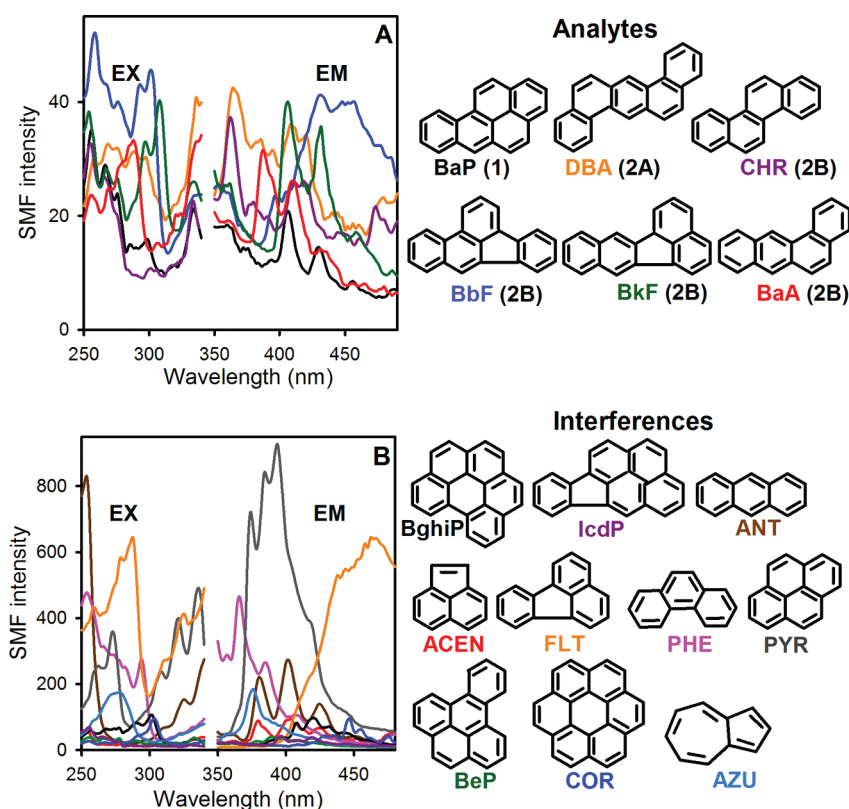


Figure 1. (A) Solid matrix fluorescence (SMF) excitation (EX) and emission (EM) spectra for BaP (black), DBA (orange), CHR (violet), BbF (blue), BkF (green), and BaA (red), and (B) for BghiP (black), IcdP (violet), ANT (brown), ACEN (red), FLT (orange), PHEN (pink), PYR (gray), BeP (green), COR (blue) and AZU (light blue) immobilized onto silica gel C18. Concentrations (all in ng L^{-1}) are: $C_{\text{BaP}} = C_{\text{BbF}} = 500$; $C_{\text{DBA}} = 1600$; $C_{\text{CHR}} = C_{\text{BkF}} = 300$; $C_{\text{BaA}} = C_{\text{BghiP}} = C_{\text{ANT}} = 1000$; $C_{\text{ACEN}} = C_{\text{PHEN}} = 1 \times 10^6$, $C_{\text{FLT}} = C_{\text{PYR}} = 1 \times 10^5$; $C_{\text{IcdP}} = C_{\text{BeP}} = 5000$; $C_{\text{COR}} = 1250$; $C_{\text{AZU}} = 6.25 \times 10^5$. The λ_{ex} (nm)/ λ_{em} (nm) are: 298/410, 268/394, 332/410, 290/454, 308/406, 290/388 for BaP, DBA, CHR, BbF, BkF, and BaA, respectively, and 300/420, 300/484, 340/402, 254/385, 288/463, 264/366, 320/394, 290/408, 304/446, and 277/377 for BghiP, IcdP, ANT, ACEN, FLT, PHEN, PYR, BeP, COR, and AZU, respectively. The IARC (International Agency for Research on cancer) carcinogenicity classification for the studied analytes is indicated in each case.

of a second injection valve. In this way, the signal returns to the baseline. The time elapsed between consecutive injections (including the fluorescence matrix measurement) was about 4 min.

Chemometric Algorithms and Software. The theory of the applied algorithms is well documented,^{7–10} and a brief description can be found in the Supporting Information. The routines employed for U-PLS, U-PLS/RBL, N-PLS, N-PLS/RBL, and PARAFAC are written in MATLAB 7.0. U-PLS, N-PLS and PARAFAC are available on the Internet.¹⁷ All algorithms were implemented using the graphical interface of the MVC2 toolbox,¹⁸ which is also available on the Internet.¹⁹

RESULTS AND DISCUSSION

Optosensing System for PAHs. Both the solid used as active material and the presence of an organic solvent in the sample (which ensures that all injected analytes reach the solid surface) are important experimental variables when a flow-through optosensor for PAHs is being implemented.¹² Because of the nonpolar nature of PAHs, and on the basis of previous experience^{4,12,13,20} nonionic solids such as Amberlite XAD-4, Amberlite XAD-7 HP, nylon 6 powder, nylon 66 powder and C18 silicagel were checked as solid-supports. While no signals were detected with any of the tested supports when pure aqueous PAH samples were injected, signals of different intensity were obtained in the presence of water-miscible organic solvents. Working samples were prepared

in different methanol, acetone, acetonitrile, and 1,4-dioxane percentages (0–70%), and were probed with the above indicated supports. The results indicated that C18 silicagel interacts with all analyzed PAHs (analytes and interferences) when the latter are dissolved in acetonitrile/water (50:50) mixtures, giving signals of significant intensities at the low assayed concentrations. In this case, the adsorbed PAHs were easily removed with a methanol solution. In conclusion, C18 silicagel was selected as solid support.

The optosensor response was found to decrease in the presence of organic solvents in the carrier stream, possibly due to an elution effect. Therefore, pure water was used as carrier (a favorable characteristic of the present system).

Figure 1A shows the fluorescence excitation and emission spectra for BaP, DBA, CHR, BbF, BkF, and BaA adsorbed on the C18 solid surface, highlighting the significant challenge implied in their simultaneous fluorimetric determination. Because the interest is focused on the analysis of real samples, the simultaneous presence of other PAHs was considered (Figure 1B), and chemometric analysis with U-PLS/RBL, N-PLS/RBL, and PARAFAC algorithms was applied to data collected for samples of increasing complexity. In a first stage, samples only containing the studied analytes were evaluated. Subsequently, more complex samples containing interferences were studied, and finally the best algorithm was applied to real environmental samples.

U-PLS and N-PLS. EEFMs were recorded for the calibration samples in a wide spectral range, involving the fluorescence signals of all studied analytes. The U-PLS model is built using the vectors obtained after unfolding the calibration data matrices and the vector of calibration concentrations, which provides a set of abstract loadings and regression coefficients. Although these latent variables do not have any physical interpretation, an adequate fit of the sample signal to the calibration model strongly indicates that the correct analyte is being quantitated. The quality of the fit is measured by appropriate statistical indicators (i.e., residual fit). The N-PLS method applied to second-order data is similar to the U-PLS method, but the original data matrices are not unfolded.

Table 1. Components Number (*A*) and Excitation–Emission Ranges Used in PLS (RBL) Methods

	U-PLS and U-PLS/RBL		N-PLS and N-PLS/RBL			
	<i>A</i>	excitation (nm)	emission (nm)	<i>A</i>	excitation (nm)	emission (nm)
BaP	3	270–320	390–450	5	280–310	400–440
DBA	4	274–300	376–470	4	270–300	380–460
CHR	4	260–280	350–460	4	250–280	360–400
BbF	2	300–340	410–490	3	300–340	400–480
BkF	3	300–340	390–470	4	290–340	400–470
BaA	4	260–300	360–450	6	250–300	350–440

The selection of both the optimum spectral range and the optimum number of factors for each studied analyte was performed applying the cross-validation method described by Haaland and Thomas to data pertaining to calibration samples only (²¹, see Supporting Information). The matrix spectral region in the proximities of one of the excitation–emission maxima for each analyte was systematically modified, selecting the parameters which rendered the best statistical indicators. Mean centering was applied for all methods, allowing to remove the effect of the background. Table 1 collects the final excitation and emission spectral ranges selected for each analyte and the corresponding number of factors when both U-PLS and N-PLS were applied.

An inspection of the number of components (*A*) estimated for U-PLS and N-PLS indicates that the former requires either equal or lesser components. Apparently, N-PLS needs additional components to correctly model the corresponding profiles. The varying number of factors may be due to the different inner structure of U-PLS and N-PLS models.

Figure 2A shows the three-dimensional plot of the EEFM for a typical validation sample (without interferences), and Figure S1 of the Supporting Information shows the prediction results for the application of U-PLS and N-PLS to the complete set of 25 validation samples, including the corresponding elliptical joint confidence region (EJCR)²² for each slope and intercept of the found vs nominal plots. The U-PLS predictions for the six calibrated PAHs are in good agreement with the nominal values,

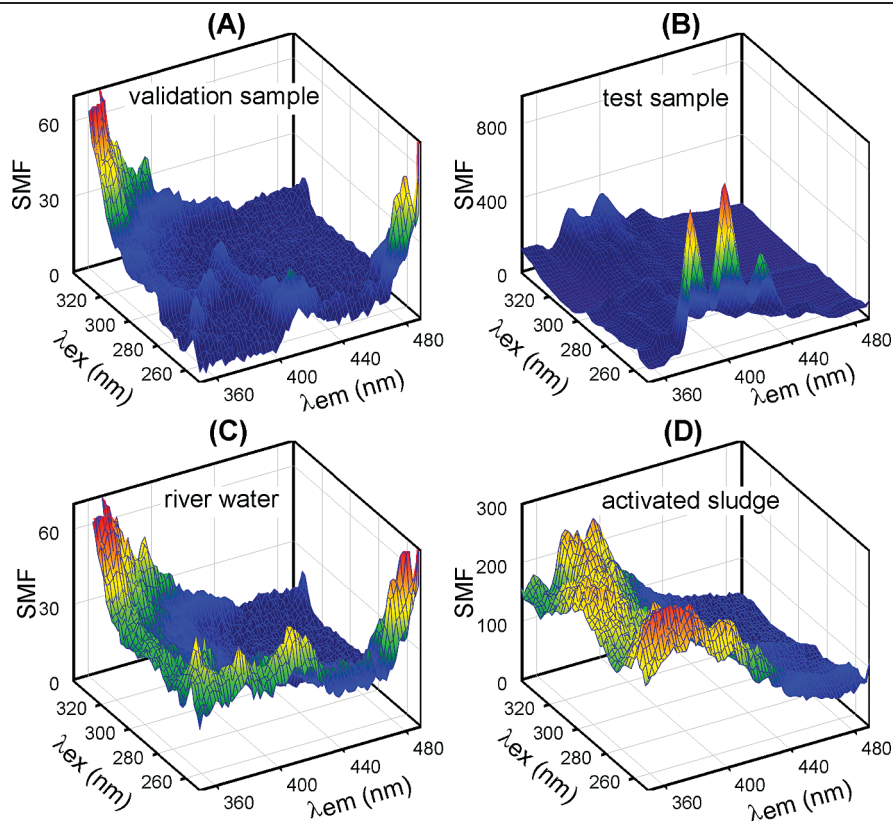


Figure 2. Three-dimensional plots for excitation–emission solid matrix fluorescence matrices corresponding to (A) a validation sample containing 120 ng L⁻¹ BaP, 600 ng L⁻¹ DBA, 170 ng L⁻¹ CHR, 130 ng L⁻¹ BbF, 200 ng L⁻¹ BkF, and 270 ng L⁻¹ BaA, (B) a test sample containing the six analytes and 750 ng L⁻¹ BghiP, 500 ng L⁻¹ IcdP, 250 ng L⁻¹ ANT, 3.75 × 10⁵ ng L⁻¹ ACEN, 3 × 10⁴ ng L⁻¹ FLT, 3.5 × 10⁵ ng L⁻¹ PHEN, 1.5 × 10⁴ ng L⁻¹ PYR, 175 ng L⁻¹ BeP, 625 ng L⁻¹ COR, and 7.5 × 10⁴ ng L⁻¹ AZU, (C) a typical river water sample, and (D) a typical activated sludge sample.

Table 2. Statistical Results for BaP, DBA, CHR, BbF, BkF, and BaA in Samples Without Interferences (Set No. 1) and with BghiP, IcdP, ANT, ACEN, FLT, PHE, PYR, BeP, COR, and AZU as Interferences (Set No. 2)^a

	U-PLS						N-PLS						PARAFAC					
	BaP	DBA	CHR	BbF	BkF	BaA	BaP	DBA	CHR	BbF	BkF	BaA	BaP	DBA	CHR	BbF	BkF	BaA
Set no. 1																		
RMSEP	14	65	51	15	17	34	23	177	74	12	10	46	37	199	81	18	16	60
REP	9	8	18	5	7	6	14	21	26	4	6	8	23	24	29	6	10	11
LOD	14	69	25	3	4	22	24	96	38	4	4	22	54	300	100	7	9	37
	U-PLS/RBL						N-PLS/RBL						PARAFAC					
Set no. 2																		
RMSEP	18	128	33	55	13	80	53	—	—	66	17	—	—	—	—	80	16	—
REP	11	15	12	20	8	14	33	—	—	24	10	—	—	—	—	29	10	—
LOD	16	115	37	6	5	57	^b	—	—	^b	^b	—	—	—	—	9	10	—

^a RMSEP (ng L^{-1}), root-mean-square error of prediction; REP (%), relative error of prediction; LOD (ng L^{-1}), limit of detection calculated according to ref 30. ^b To the best of our knowledge, there are no reports on the estimation of the LOD for the N-PLS/RBL method.

and the ellipses include the theoretically expected values of slope = 1 and intercept = 0, indicating the accuracy of the used methodology. On the other hand, N-PLS yields good results for BbF, BkF, and BaA, but a poorer precision for BaP, DBA, and CHR. These three analytes have low quantum efficiency in the silica gel C18 support. As is apparent, their determination with N-PLS is difficult. These conclusions are in agreement with the relative error of prediction (REP) values shown in Table 2.

In relation to the limits of detection (LODs), it is first necessary to consider the low concentration levels of PAHs admitted by governmental agencies in environmental samples, especially water. The European Community Council indicates that the maximum admissible concentration level for PAHs in surface water is 200 ng L^{-1} , except for the BaP level, which is decreased to 20 ng L^{-1} .²³ USEPA reports a value of 200 ng L^{-1} as a maximum concentration level for PAHs in safe drinking water.²⁴

The best LODs, which are in the order of 4 ng L^{-1} , are achieved for BbF and BkF using both PLS algorithms. The low LOD obtained for the most carcinogenic PAH (BaP) when U-PLS is applied ($\text{LOD} = 14 \text{ ng L}^{-1}$) is very favorable, taking into account the complexity of the system evaluated and the simplicity of the determination. Although the highest LOD is obtained for DBA (second in the carcinogenic list), this value (below 100 parts per trillion) can be considered acceptable for the determination of DBA in potentially contaminated samples.

The determination of the six heavy PAHs in the presence of other fluorescent PAHs was evaluated in 36 test samples containing BghiP, IcdP, ANT, ACEN, FLT, PHEN, PYR, BeP, COR, and AZU as potential interferences. Figure 1B shows the fluorescence spectra of the latter ten selected PAHs adsorbed in the solid support, where a significant overlapping among them and those for the studied analytes can be observed. It is also apparent in this figure that the interferences were analyzed at high concentrations, in order to maximize the problem they may cause in the determination.

Figure 2B shows a three-dimensional plot of the EEFM for a typical sample containing the studied analytes and the 10 PAH interferences. The real challenge we are facing is apparent when comparing the latter figure and Figure 2A, which shows the analytes EEFM plot for a mixture of analytes without interferences. When U- and N-PLS/RBL were applied to these test samples, in addition to the latent variables estimated for each

analyte from the calibration set, they required the introduction of the RBL procedure with an additional number of components corresponding to the unexpected sample constituents. This number, estimated by suitable consideration of RBL residues,⁴ ranged from 1 to 5, depending on the analyzed PAH and the corresponding spectral range.

Figure 3 shows the prediction results corresponding to the application of U-PLS/RBL and N-PLS/RBL to the samples containing interferences. As can be observed, the ability of U-PLS/RBL to resolve highly overlapped analytes is preserved, even in a very interfering medium. Although all ellipses include the theoretical (1,0) point, the calculated values for BbF show some dispersion with respect to the perfect fit line. The obtained values for BbF, which are worse than those obtained in samples without interferences, could be ascribed to the presence of FLT as interference, whose spectra seriously overlap with those for BbF (see Figure 1). On the other hand, N-PLS was only able to successfully predict the concentrations of BaP, BbF, and BkF. This demonstrates, as in previous related works,^{4,20} a weaker capability of this algorithm to resolve this type of complex systems.

PARAFAC. This algorithm was applied to the same set of 25 validation samples examined by both PLS algorithms. Exploratory experiments showed that the optimum matrix spectral ranges for each analyte when PARAFAC was applied were similar to those selected for N-PLS analysis (Table 1). In contrast to PLS, the PARAFAC model allows to obtain physically interpretable profiles. Identification of the chemical constituents under investigation is done with the aid of the estimated profiles, and comparing them with those for a standard solution of the analyte of interest. The number of responsive components, selected by the so-called core consistency analysis,²⁵ was 5, 5, 5, 4, 4, and 4 for BaP, DBA, CHR, BbF, BkF, and BaA, respectively. These numbers may differ from those required by PLS methods because of the need of modeling the data in terms of physically interpretable PARAFAC components. The results for BbF, BkF, and BaA (Supporting Information Figure S2) are in good agreement with the nominal values, while the predictions for the remaining calibrated compounds are more disperse, although the corresponding elliptical tests are acceptable. These observations agree with the statistical values shown in Table 2.

When PARAFAC was applied to the samples in the presence of interferences, only the concentrations of BbF and BkF, which

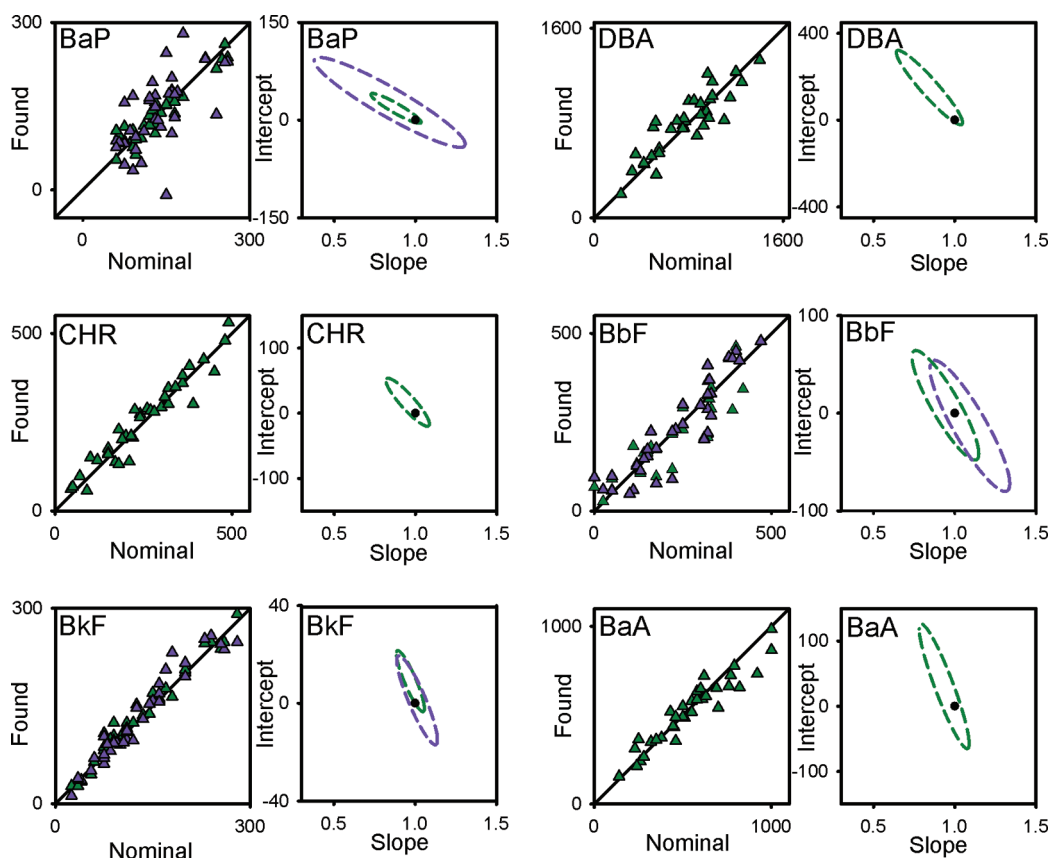


Figure 3. Plots for U-PLS (green triangles) and N-PLS (violet triangles) predicted concentrations as a function of the nominal values for BaP, DBA, CHR, BbF, BkF, and BaA in samples with interferences as indicated, and the corresponding elliptical joint regions (at 95% confidence level) for the slopes and intercepts of the regressions for U-PLS (green dashed lines) and N-PLS (violet dashed lines) predictions. Black circles in the elliptical plots mark the theoretical (intercept = 0, slope = 1) point.

Table 3. Determination of the PAH Concentrations in River Waters^a

	sample 1		sample 2		sample 3		sample 4		sample 5	
	GC/MS	U-PLS/RBL ^b	GC/MS	U-PLS/RBL ^b	GC/MS	U-PLS/RBL ^b	GC/MS	U-PLS/RBL ^b	GC/MS	U-PLS/RBL ^b
BaP	50	51 (1)	50	49 (3)	65	65 (2)	50	47 (4)	15	24 (2)
DBA	230	230 (10)	175	226 (10)	215	226 (4)	230	270 (10)	275	275 (3)
CHR	110	132 (1)	150	151 (4)	95	84 (8)	110	112 (9)	125	89 (10)
BbF	90	104 (2)	60	11 (1)	45	47 (2)	90	99 (10)	110	103 (5)
BkF	20	14 (5)	25	30 (3)	70	69 (1)	20	5 (2)	58	77 (1)
BaA	50	60 (3)	80	111 (10)	110	72 (6)	50	64 (3)	120	127 (3)

^a ng L⁻¹. ^b Mean of duplicates. Standard deviation between parentheses.

produce the highest fluorescence signals, could be predicted with relative precision (Supporting Information Figure S2). The poor results obtained with PARAFAC for BaP, DBA, CHR, and BaA may be ascribed to a lack of selectivity for these analytes. Indeed, the significant spectral overlapping among analytes and interferences appears to preclude the successful decomposition of the second-order data.²⁶

River and Activated Sludge Samples. According to the obtained results with artificial samples, U-PLS/RBL was selected as the algorithm of choice for the analysis of real samples.

Two very different types of samples (water samples taken from a river at places near local industries and activated sludge samples) were selected as examples of real matrices for assaying the proposed

methodology. The concentrations of the six studied PAHs in each sample were first determined by a reference method (GC-MS).

Figure 2C and D show three-dimensional plots of the EEFM corresponding to one of the studied water samples and for a typical activated sludge sample, respectively. Table 3 shows that the results supplied by the presently proposed strategy using U-PLS/RBL for the water samples are similar to those obtained with GC-MS, and that the PAH levels in these waters are slightly higher than those allowed by regulatory agencies.^{23,24}

Table 4 shows the obtained values for the activated sludge samples. Activated sludge is a usual treatment for removing PAHs and other organic compounds from industrial waste waters, using air and a biological floc composed of bacteria and

Table 4. Determination of the PAH Concentrations in Activated Sludges^a

	sample 1		sample 2		sample 3		sample 4		sample 5	
	GC/MS	U-PLS/RBL ^b	GC/MS	U-PLS/RBL ^b	GC/MS	U-PLS/RBL ^b	GC/MS	U-PLS/RBL ^b	GC/MS	U-PLS/RBL ^b
BaP	0.40	0.41 (0.06)	0.83	0.77 (0.06)	0.30	0.20 (0.07)	0.53	0.55 (0.03)	0.50	0.52 (0.03)
DBA	1.50	1.88 (0.07)	4.33	4.58 (0.01)	1.07	1.16 (0.09)	2.50	2.18 (0.08)	2.00	3.0 (0.2)
CHR	0.83	0.68 (0.07)	0.86	1.5 (0.1)	0.84	0.8 (0.2)	0.60	0.8 (0.2)	2.50	2.55 (0.01)
BbF	1.17	1.2 (0.1)	0.67	0.54 (0.03)	0.33	0.24 (0.03)	0.70	0.7 (0.3)	0.53	0.55 (0.02)
BkF	0.50	0.6 (0.1)	0.22	0.26 (0.02)	0.50	0.99 (0.02)	0.67	0.3 (0.1)	0.30	0.3 (0.1)
BaA	1.50	2.15 (0.06)	1.83	1.99 (0.09)	2.50	2.35 (0.08)	1.50	1.9 (0.4)	2.67	2.56 (0.08)

^a mg kg⁻¹ of dry mass. ^b Mean of duplicates. Standard deviation between parentheses.

protozoans. These sludges represent an inexpensive nutrient source in agriculture and are frequently used as fertilizers and soil conditioners.²⁷ However, the quality of the final product must be guaranteed in order to avoid the possible bioavailability of persistent toxic compounds such as PAHs. The accepted European Union limits for the total concentration of 11 concerned PAHs in sludge for agricultural use is 6.0 mg kg⁻¹.²⁷ The maximum level admitted for the U.S. legislation is 4.6 mg kg⁻¹ (calculated as the sum of seven heavy-PAHs) but concentrations larger than 1 mg kg⁻¹ for BaP are not allowed.²⁸

Taking into account that the low weight PAHs are more rapidly biodegraded, and that the PAH content is basically given by heavy-PAHs, one can assess that only samples 1 and 3 (Table 4) can be considered safe for agricultural purposes, at least from the point of view of the PAH content.

The statistical comparison between the obtained results and those provided by the reference method in both sets of samples was carried out by the EJCR test for the slope and intercept of the found vs reference concentrations plot. According to Martínez et al., the elliptical region was calculated considering the experimental data corresponding to all analytes, in order to better estimate the prediction variance.²⁹ This avoids the oversizing of the joint confidence region due to large experimental random errors and thus the probability of not detecting the presence of bias. Due to widely different PAH contents in both set of samples (water and sludge), this ellipse was constructed from the concentration values predicted in the experimental cell for each analyte. The obtained ellipse (Figure S3 of the Supporting Information) includes the theoretically expected (1,0) point, supporting that the results obtained with the method here proposed are statistically comparable with those provided by the reference one.

Finally, the advantages of the proposed methodology in comparison with GC-MS were apparent in the treatment of real samples: (1) lower experimentally required time (4 min per sample vs 60 min per sample), (2) higher sensitivity (part per trillion levels vs part per million levels), and (3) considerably more simplicity.

■ ASSOCIATED CONTENT

Supporting Information. Quality assurance information, a brief explanation of the theories of U-PLS/RBL, N-PLS/RBL and PARAFAC, and additional figures. This material is available free of charge via the Internet at <http://pubs.acs.org>.

■ AUTHOR INFORMATION

Corresponding Author

*E-mail: escandar@iquir-conicet.gov.ar; phone: +54-341-4372704; fax: +54-341-4372704.

■ ACKNOWLEDGMENT

Financial support for this research was provided by Universidad Nacional de Rosario, CONICET (Consejo Nacional de Investigaciones Científicas y Técnicas, Project PIP 1950), and ANPCyT (Agencia Nacional de Promoción Científica y Tecnológica, Project PAE-22204).

■ REFERENCES

- Wenzl, T.; Simon, R.; Kleiner, J.; Anklam, E. Analytical methods for polycyclic aromatic hydrocarbons (PAHs) in food and the environment needed for new food legislation in the European Union. *Trends Anal. Chem.* **2006**, *25*, 716–725.
- Integrated Risk Information System (IRIS). <http://www.epa.gov/iris/index.html> (accessed December 2010).
- IARC Monographs on the Evaluation of Carcinogenic Risks to Humans. <http://monographs.iarc.fr/ENG/Classification/> (accessed December 2010).
- Bortolato, S. A.; Arancibia, J. A.; Escandar, G. M. Chemometrics-assisted excitation-emission fluorescence spectroscopy on nylon membranes. Simultaneous determination of benzo[*a*]pyrene and dibenz[*a,h*]anthracene at parts-per-trillion levels in the presence of the remaining EPA PAH priority pollutants as interferences. *Anal. Chem.* **2008**, *80*, 8276–8286.
- Olivieri, A. C. Analytical advantages of multivariate data processing. One, two, three, infinity? *Anal. Chem.* **2008**, *80*, 5713–5720.
- Mas, S.; de Juan, A.; Tauler, R.; Olivieri, A. C.; Escandar, G. M. Application of chemometric methods to environmental analysis of organic pollutants: A review. *Talanta* **2010**, *80*, 1052–1067.
- Öhman, J.; Geladi, P.; Wold, S. Residual bilinearization. Part 1: Theory and algorithms. *J. Chemom.* **1990**, *4*, 79–90.
- Olivieri, A. C. On a versatile second-order multivariate calibration method based on partial least-squares and residual bilinearization. Second-order advantage and precision properties. *J. Chemom.* **2005**, *19*, 253–265.
- Bro, R. Multiway calibration. Multilinear PLS. *J. Chemom.* **1996**, *10*, 47–61.
- Bro, R. PARAFAC. Tutorial and applications. *Chemom. Intell. Lab. Syst.* **1997**, *38*, 149–171.
- Matsuoka, S.; Yoshimura, K. Recent trends in solid phase spectrometry: 2003–2009. A Review. *Anal. Chim. Acta* **2010**, *664*, 1–18.
- Fernández Sánchez, J. F.; Segura Carretero, A.; Cruces Blanco, C.; Fernández Gutiérrez, A. The development of solid-surface fluorescence characterization of polycyclic aromatic hydrocarbons for potential screening tests in environmental samples. *Talanta* **2003**, *60*, 287–293.
- Fernández Sánchez, J. F.; Segura Carretero, A.; Benítez Sánchez, J. M.; Cruces Blanco, C.; Fernández Gutiérrez, A. Fluorescence optosensor using an artificial neural network for screening of polycyclic aromatic hydrocarbons. *Anal. Chim. Acta* **2004**, *510*, 183–187.
- Salinas Castillo, A.; Fernández Sánchez, J. F.; Segura Carretero, A.; Fernández Gutiérrez, A. Solid-surface phosphorescence characterization of polycyclic aromatic hydrocarbons and selective determination of benzo[*a*]pyrene in water samples. *Anal. Chim. Acta* **2005**, *550*, 53–60.

- (15) Traviesa Alvarez, J. M.; Sánchez Barragán, I.; Costa Fernández, J. M.; Pereiro, R.; Sanz Medel, A. Room temperature phosphorescence optosensing of benzo(a)pyrene in water using halogenated molecularly imprinted polymers. *Analyst* **2007**, *132*, 218–223.
- (16) Chen, Y.; Zhu, L.; Zhou, R. Characterization and distribution of polycyclic aromatic hydrocarbon in surface water and sediment from Qiantang River, China. *J. Hazard. Mater.* **2007**, *141*, 148–155.
- (17) Algorithms and Source Code. <http://www.models.kvl.dk/source/> (accessed December 2010).
- (18) Olivieri, A. C.; Wu, H. L.; Yu, R. Q. MVC2: A MATLAB graphical interface toolbox for second-order multivariate calibration. *Chemom. Intell. Lab. Syst.* **2009**, *96*, 246–251.
- (19) Chemometry Consultancy. www.chemometry.com (accessed December 2010).
- (20) Piccirilli, G. N.; Escandar, G. M. Second-order advantage with excitation-emission fluorescence spectroscopy and a flow-through optosensing device. Simultaneous determination of thiabendazole and fubridazole in the presence of uncalibrated interferences. *Analyst* **2010**, *135*, 1299–1308.
- (21) Haaland, D. M.; Thomas, E. V. Partial least-squares methods for spectral analyses. 1. Relation to other quantitative calibration methods and the extraction of qualitative information. *Anal. Chem.* **1988**, *60*, 1193–1202.
- (22) González, A. G.; Herrador, M. A.; Asuero, A. G. Intra-laboratory testing of method accuracy from recovery assays. *Talanta* **1999**, *48*, 729–736.
- (23) Ferrer, R.; Beltrán, J. L.; Guiteras, J. Use of cloud point extraction methodology for the determination of PAHs priority pollutants in water samples by high-performance liquid chromatography with fluorescence detection and wavelength programming. *Anal. Chim. Acta* **1996**, *330*, 199–206.
- (24) Technical Factsheet on: POLYCYCLIC AROMATIC HYDROCARBONS (PAHs). <http://www.epa.gov/safewater/pdfs/factsheets/soc/tech/pahs.pdf> (accessed December 2010).
- (25) Bro, R.; Kiers, H. L. A. A new efficient method for determining the number of components in PARAFAC models. *J. Chemom.* **2003**, *17*, 274–286.
- (26) Arancibia, J. A.; Olivieri, A. C.; Escandar, G. M. First- and second-order multivariate calibration applied to biological samples: determination of anti-inflammatories in serum and urine. *Anal. Bioanal. Chem.* **2002**, *374*, 451–459.
- (27) Hafidi, M.; Amir, S.; Jouraiphy, A.; Winterton, P.; El Gharous, M.; Merlina, G.; Revel, J. C. Fate of polycyclic aromatic hydrocarbons during composting of activated sewage sludge with green waste. *Bioresour. Technol.* **2008**, *99*, 8819–8823.
- (28) Villar, P.; Callejón, M.; Alonso, E.; Jiménez, J. C.; Guiraúm, A. Temporal evolution of polycyclic aromatic hydrocarbons (PAHs) in sludge from wastewater treatment plants: Comparison between PAHs and heavy metals. *Chemosphere* **2006**, *64*, 535–541.
- (29) Martínez, A.; Riu, J.; Busto, O.; Guasch, J.; Rius, F. X. Validation of bias in multianalyte determination methods. Application to RP-HPLC derivatizing methodologies. *Anal. Chim. Acta* **2000**, *406*, 257–278.
- (30) Boqué, R.; Larrechi, M. S.; Rius, F. X. Multivariate detection limits with fixed probabilities of error. *Chemom. Intell. Lab. Syst.* **1999**, *45*, 397–408.